

Understanding the role of eco-evolutionary feedbacks in host-parasite coevolution

Citation for published version:

Ashby, B, Iritani, R, Best, A, White, A & Boots, M 2019, 'Understanding the role of eco-evolutionary feedbacks in host-parasite coevolution', *Journal of Theoretical Biology*, vol. 464, pp. 115-125.
<https://doi.org/10.1016/j.jtbi.2018.12.031>

Digital Object Identifier (DOI):

[10.1016/j.jtbi.2018.12.031](https://doi.org/10.1016/j.jtbi.2018.12.031)

Link:

[Link to publication record in Heriot-Watt Research Portal](#)

Document Version:

Peer reviewed version

Published In:

Journal of Theoretical Biology

General rights

Copyright for the publications made accessible via Heriot-Watt Research Portal is retained by the author(s) and / or other copyright owners and it is a condition of accessing these publications that users recognise and abide by the legal requirements associated with these rights.

Take down policy

Heriot-Watt University has made every reasonable effort to ensure that the content in Heriot-Watt Research Portal complies with UK legislation. If you believe that the public display of this file breaches copyright please contact open.access@hw.ac.uk providing details, and we will remove access to the work immediately and investigate your claim.

Supplementary material: Understanding the role of eco-evolutionary feedbacks in host-parasite coevolution

S1. Details of the literature analysis

We searched the PubMed database using the following query:

(model* OR simulation* OR theory OR theoretical OR mathematical) AND (coevolution* OR co-evolution* OR coevolve* OR co-evolve* OR (red AND queen)) AND (host* OR parasite* OR pathogen*) AND ("2000"[Date - Publication] : "2017"[Date - Publication]).

The search returned a total of 1058 studies, 9 of which were removed from further analysis due to erroneous publication dates. Of the remaining 1049 studies, 185 were found to include a theoretical model of host-parasite coevolution (determined through manual inspection of each study). These studies were then categorised according to whether both host and parasite populations were dynamic or if one or more population size was fixed (summary results in Table S1). Raw search data and breakdown of the analysis are shown in a separate file.

Publication year	Number of studies	Percentage of studies without host and/or parasite population dynamics
2000	4	75.00%
2001	3	66.67%
2002	5	40.00%
2003	10	50.00%
2004	3	100.00%
2005	6	66.67%
2006	6	83.33%
2007	10	90.00%
2008	8	62.50%
2009	16	56.25%
2010	6	33.33%
2011	7	57.14%
2012	12	66.67%
2013	15	53.33%
2014	17	47.06%
2015	18	27.78%
2016	12	41.67%
2017	25	44.00%
Total	183	75.00%

Table S1 – Results of the literature analysis.

S2. Stability analysis for the single locus model

The fitness functions for the single locus model are given by equation (6) in the main text. The population and evolutionary dynamics are given by:

$$\frac{dH}{dt} = \bar{m}_H H \quad (S1a)$$

$$\frac{dP}{dt} = \bar{m}_P P \quad (S1b)$$

$$\frac{dh}{dt} = h(m_1^H - \bar{m}_H) \quad (S1c)$$

$$\frac{dp}{dt} = p(m_1^P - \bar{m}_P) \quad (S1d)$$

In the absence of eco-evolutionary feedbacks, the evolutionary dynamics are independent of equations (S1a-b), in which case the Jacobian is:

$$J = \begin{pmatrix} (1-2h)(m_1^H - m_2^H) & h(1-h)\left(\frac{\partial m_1^H}{\partial p} - \frac{\partial m_2^H}{\partial p}\right) \\ p(1-p)\left(\frac{\partial m_1^P}{\partial h} - \frac{\partial m_2^P}{\partial h}\right) & (1-2p)(m_1^P - m_2^P) \end{pmatrix} \quad (S2)$$

In the matching allele model, the internal equilibrium occurs at $(h^*, p^*) = (\frac{1}{2}, \frac{1}{2})$. The leading diagonal elements of J therefore disappear and the eigenvalues are:

$$\lambda = \pm \frac{1}{4} \sqrt{\left(\frac{\partial m_1^H}{\partial p} - \frac{\partial m_2^H}{\partial p}\right)\left(\frac{\partial m_1^P}{\partial h} - \frac{\partial m_2^P}{\partial h}\right)} \quad (S3)$$

with the derivatives evaluated at (h^*, p^*) . The terms $\left(\frac{\partial m_1^H}{\partial p} - \frac{\partial m_2^H}{\partial p}\right)$ and $\left(\frac{\partial m_1^P}{\partial h} - \frac{\partial m_2^P}{\partial h}\right)$ have opposite signs, which means the eigenvalues are imaginary and hence the system exhibits neutrally stable cycles.

In the gene-for-gene model with costs the internal equilibrium, which exists for $\beta_H > c_H$, occurs at

$$(h^*, p^*) = \left(1 - c_P, \frac{c_H(1 - \beta_H(1 - c_P))}{\beta_H(1 - c_H(1 - c_P))}\right) \quad (S4)$$

and the eigenvalues are

$$\lambda = \pm \sqrt{\frac{c_H c_P \beta_P (1 - c_P) (c_H - \beta_H) (1 - (1 - c_P) \beta_H)}{\beta_H (1 - c_H (1 - c_P))}} \quad (S5)$$

which are imaginary and hence this system also exhibits neutrally stable cycles.

We now introduce eco-evolutionary feedbacks by setting $z_H(P) = P$ and $z_P(H) = H$ in equation (6) in the main text. This means that the evolutionary dynamics of equation (S1c-d) depend on the ecological dynamics in equation (S1a-b). The Jacobian is then given by:

$$J = \begin{pmatrix} J_{11} & J_{12} \\ J_{21} & J_{22} \end{pmatrix} \quad (S6)$$

where

$$J_{11} = \begin{pmatrix} H \left(h \frac{\partial m_1^H}{\partial H} + (1 - h) \frac{\partial m_2^H}{\partial H} \right) + h m_1^H + (1 - h) m_2^H & H \left(h \frac{\partial m_1^H}{\partial P} + (1 - h) \frac{\partial m_2^H}{\partial P} \right) \\ P \left(p \frac{\partial m_1^P}{\partial H} + (1 - p) \frac{\partial m_2^P}{\partial H} \right) & P \left(p \frac{\partial m_1^P}{\partial P} + (1 - p) \frac{\partial m_2^P}{\partial P} \right) + p m_1^P + (1 - p) m_2^P \end{pmatrix} \quad (S7a)$$

$$J_{12} = \begin{pmatrix} H(m_1^H - m_2^H) & H \left(h \frac{\partial m_1^H}{\partial p} + (1 - h) \frac{\partial m_2^H}{\partial p} \right) \\ P \left(p \frac{\partial m_1^P}{\partial h} + (1 - p) \frac{\partial m_2^P}{\partial h} \right) & P(m_1^P - m_2^P) \end{pmatrix} \quad (S7b)$$

$$J_{21} = \begin{pmatrix} h(1 - h) \left(\frac{\partial m_1^H}{\partial H} - \frac{\partial m_2^H}{\partial H} \right) & h(1 - h) \left(\frac{\partial m_1^H}{\partial P} - \frac{\partial m_2^H}{\partial P} \right) \\ p(1 - p) \left(\frac{\partial m_1^P}{\partial H} - \frac{\partial m_2^P}{\partial H} \right) & p(1 - p) \left(\frac{\partial m_1^P}{\partial P} - \frac{\partial m_2^P}{\partial P} \right) \end{pmatrix} \quad (S7c)$$

and J_{22} is equal to equation (S2).

In the matching allele model, the internal equilibrium occurs at

$$(H^*, P^*, h^*, p^*) = \left(\frac{4q_P}{\beta_H \beta_P + 4q_H q_P}, \frac{2\beta_P}{\beta_H \beta_P + 4q_H q_P}, \frac{1}{2}, \frac{1}{2} \right) \quad (S8)$$

at which point the matrices J_{12} and J_{21} are zero. The eigenvalues are given by:

$$\lambda_{1,2} = \frac{-q_P(\beta_P + 2q_H) \pm 2 \sqrt{q_P \left(q_P \left(q_H - \frac{\beta_P}{2} \right)^2 - \frac{\beta_H \beta_P^2}{2} \right)}}{\beta_H \beta_P + 4q_H q_P} \quad (S9a)$$

$$\lambda_{3,4} = \pm \frac{\beta_P \sqrt{-2q_H \beta_H}}{\beta_H \beta_P + 4q_H q_P} \quad (S9b)$$

The first two eigenvalues, $\lambda_{1,2}$, correspond to the ecological dynamics near the internal equilibrium, and the latter two, $\lambda_{3,4}$, to the coevolutionary dynamics. Since $\lambda_{3,4}$ are imaginary, this implies that the long-term coevolutionary dynamics are neutrally stable cycles. However, the ecological dynamics are stabilising, which ultimately has a damping effect on the amplitude of the coevolutionary cycles until the population densities reach equilibrium (Fig. 2B).

In the gene-for-gene model, the internal equilibrium, (H^*, P^*, h^*, p^*) , occurs at

$$\left(\frac{q_P(1 - c_H)}{K_0}, \frac{\beta_P(1 - c_H)(1 - c_P)}{K_0}, 1 - c_P, \frac{c_H q_H q_P}{\beta_H \beta_P (1 - c_H)(1 - c_P)} \right) \quad (\text{S10})$$

where $K_0 = \beta_P(1 - c_P)^2(1 - c_H)\beta_H + q_H q_P(1 - c_H(1 - c_P))$. Substituting in the parameter values from Fig. 2, we find that all 4 eigenvalues are complex with negative real parts. Since the first two eigenvalues correspond to the ecological dynamics and the latter two to the evolutionary dynamics, this means that both exhibit damped cycles, as shown in Fig. 2D.

S3. Non-linear encounter probabilities

In the main text we assume that the encounter probability functions, $z_H(P)$ and $z_P(H)$, which are used to introduce eco-evolutionary feedbacks to the models, vary linearly with population density. Here, we show that the effects are broadly similar when these functions are non-linear by setting:

$$z_H(P) = a_P \left(\frac{P}{P_{max}} \right)^{b_P} + (1 - a_P) \quad (\text{S11a})$$

$$z_P(H) = a_H \left(\frac{H}{H_{max}} \right)^{b_H} + (1 - a_H) \quad (\text{S11b})$$

where $b_H > 0$ and $b_P > 0$ control the shape of the relationships between relative population density and encounter rate. Using these functions, we run simulations as described in the main text for the multi-locus (Fig. S1) and quantitative trait (Fig. S2) models (compare with Fig. 3B and Fig. 6A, 6C, respectively).

Supplementary material:
Understanding the role of eco-evolutionary feedbacks in host-parasite coevolution

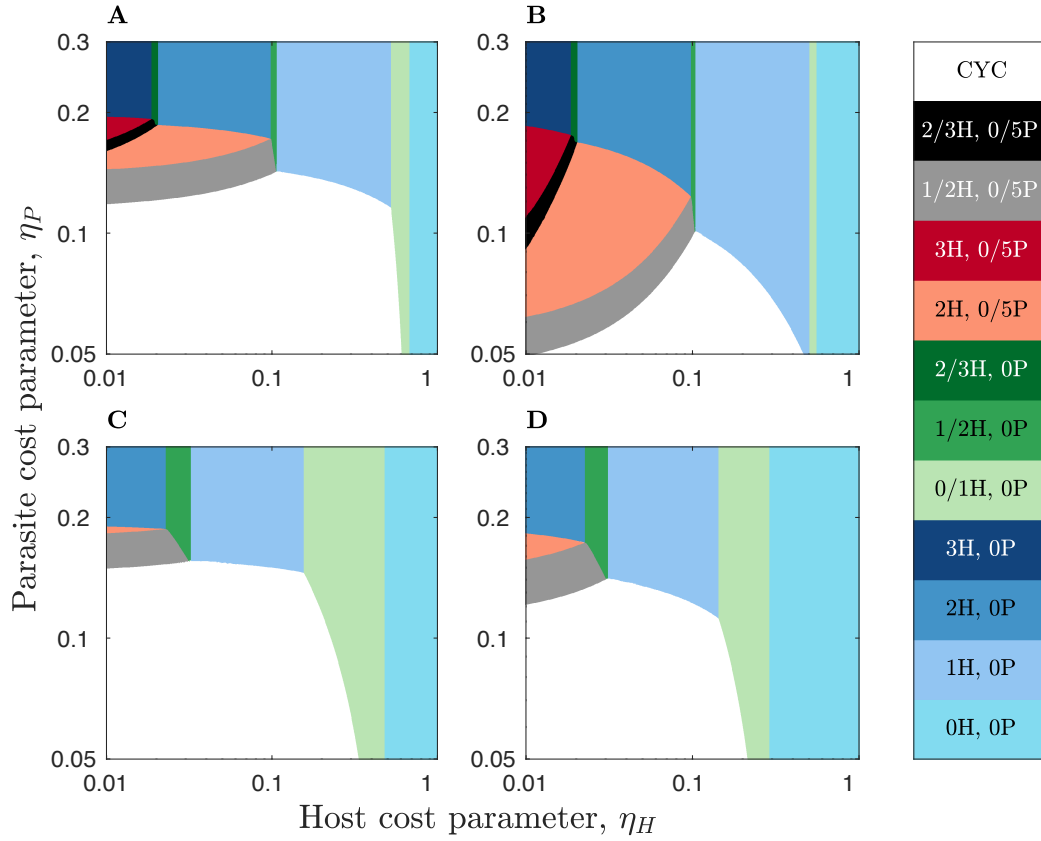


Figure S1 – Effects of eco-evolutionary feedbacks on the multilocus gene-for-gene model of host-parasite coevolution described in the main text, with non-linear encounter probabilities (equation S11). Qualitatively similar outcomes are grouped by colour: blues = trait monomorphism in both populations; greens = polymorphic host traits only; reds = polymorphic parasite traits only; grey/black = both polymorphic; white = cycling. The key shows the level of investment in the host and parasite (e.g. “2/3H, 0/5P” means that hosts with 2 or 3 alleles coexist with parasites that have 0 or 5 alleles). Eco-evolutionary feedbacks facilitate trait polymorphism and generally reduce the propensity for coevolutionary cycling. Other parameters: $a_H, a_P = 1$, $\beta_H, \beta_P = 1$, $L = 5$, $\tilde{q}_H = 1$, $\tilde{q}_P = e^{\beta_P}$, $\sigma = 0.2$, and: (A) $b_H = 0.5, b_P = 0.5$; (B) $b_H = 2, b_P = 0.5$; (C) $b_H = 2, b_P = 0.5$; (D) $b_H = 2, b_P = 2$.

Supplementary material:
Understanding the role of eco-evolutionary feedbacks in host-parasite coevolution

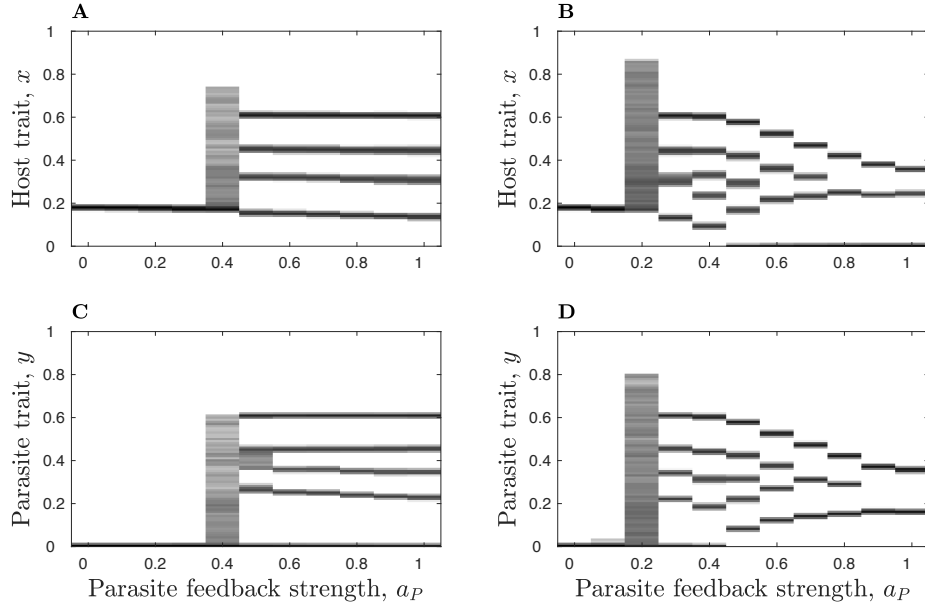


Figure S2 – Analysis of the quantitative trait model with non-linear encounter probabilities (equation S11). Hosts and parasites vary in their degree of specialism, as described in Fig. 6. Panels (A) and (B) show the mean frequency of host traits and panels (C) and (D) show the mean frequency of parasite traits (following a burn-in period) as the strength of the parasite feedback is varied. Parameters and cost functions as described for Fig. 6, with $b_H = 1$ and: (A, C) $b_P = 1/3$; (B, D) $b_P = 3$.

Supplementary material:
Understanding the role of eco-evolutionary feedbacks in host-parasite coevolution

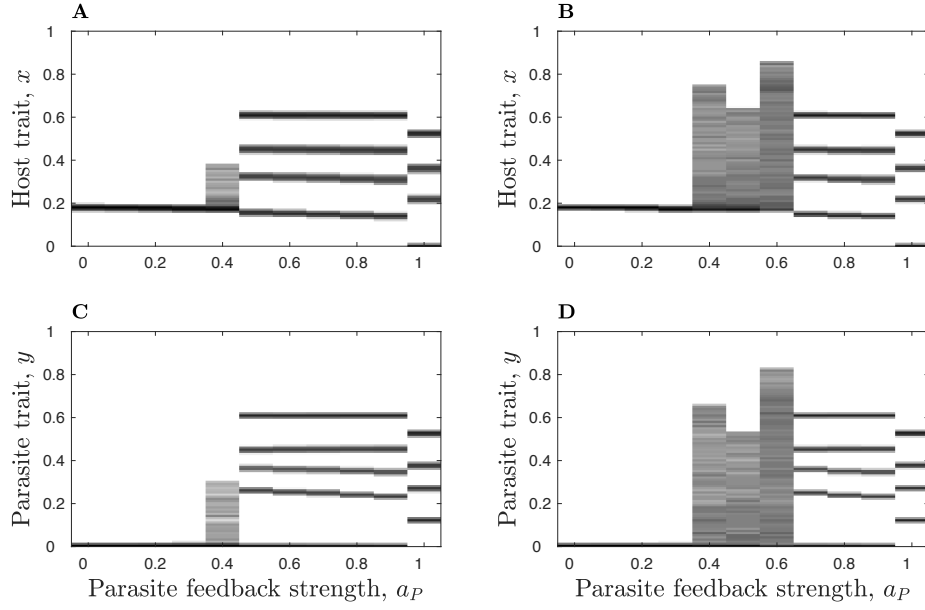


Figure S3 – Analysis of the quantitative trait model with linear encounter probabilities and (A,C) faster or (B, D) slower mutation rates. Hosts and parasites vary in their degree of specialism, as described in Fig. 6. Panels (A) and (B) show the mean frequency of host traits and panels (C) and (D) show the mean frequency of parasite traits (following a burn-in period) as the strength of the parasite feedback is varied. Parameters and cost functions as described for Fig. 6, with $b_H = 1$, $b_P = 1/3$ and: (A, C) $T = 500$; (B, D) $T = 2000$.